This article has been accepted for publication in a future issue of this journal, but has not been fully edited. Content may change prior to final publication. Citation information: DOI 10.1109/TPEL.2020.3009619, IEEE Transactions on Power Electronics

An improved voltage-shifting strategy to attain concomitant accurate power sharing and voltage restoration in droop-controlled dc microgrids

Waner Wodson A. G. Silva, *Student Member, IEEE,*, Thiago R. Oliveira, *Member, IEEE,* and Pedro F. Donoso-Garcia

***Abstract*—This work proposes a distributed secondary level control strategy for dc microgrids, which achieves accurate and proportional power sharing and dc bus voltage deviation restoration based on voltage-shifting. In contrast to similar approaches, only one variable per converter is transmitted in the low-bandwidth communication link and with a simple integrator as the secondary level controller both objectives are achieved simultaneously. The information state shared between converters is a λ factor that incorporates the converter output voltage and power information. The secondary control computes the average λ locally and the controller generates an unique voltage-shifting term that modifies the converter output voltage reference. When all converters' λ converge to the average value, both proportional power sharing and dc bus voltage restoration are attained. The proposed technique suppresses the need for a complex control structure and large amount of converter variables. The proposed control is evaluated through PLECS simulation and it is validated in a 6.4 kW dc microgrid setup.**

***Index Terms*—DC microgrid, accurate power sharing, voltage restoration, voltage-shifiting, distributed control.**

I. Introduction

THE microgrid (μG) concept is a solution for the integration of multiple renewable energy sources and energy storage systems into the grid, enabling local resources to be clustered together and operate either islanded or grid-tied, thus providing more flexibility and resilience to the electrical system [1]–[3]. Recently, DC-μGs have become more prominent due to their advantages over AC-μGs [4], e.g., simplified power control, since there is no reactive power flow, phase synchronization and ac power quality issues [5], [6]. Moreover, since most renewable sources and storage devices exhibit a dc output, interfacing them to the main bus of a DC-μG requires less power conversion stages, thus leading to a more efficient approach [4], [5], [7], [8].

Fig. 1 depicts a typical DC-μG architecture for buildings, along with its main elements: a Bidirectional Interface Converter (BIC), which is responsible for interfacing the main dc bus and the utility grid at a point of common coupling (PCC), a Renewable Resource Interface Converter (RRC) and an Energy Storage Interface Converter (ESC), which are responsible for interfacing the distributed generation and storage to the dc bus, respectively. Another common element to μGs is the communication network, which is generally used to implement a hierarchical control strategy that operates at different time scales to achieve multiple control goals [3]. A 380 V dc bus is the system backbone, interlinking all μG converters and loads. The μG's control is divided into layers, where the primary layer is commonly implemented with a droop technique to achieve decentralized power sharing, high reliability, flexibility, expandability and *plug-and-play* capability for the DC-μG [3], [9]–[11]. The secondary control layer is responsible for ensuring that the electrical values of the μG are within predefined ranges, thus providing means for correcting errors eventually introduced by the primary layer [1], [12].

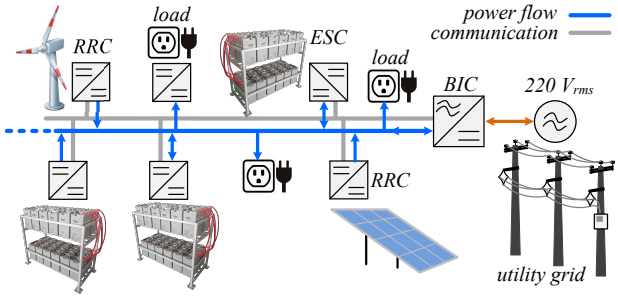

Fig. 1. DC microgrid for buildings.

In spite of its advantages, droop control has limitations such as the existence of a trade-off between tight voltage regulation and accurate power sharing as well as power sharing being strongly influenced by line impedances [11], [13]–[15]. In order to compensate the dc bus voltage deviation and to correct power imbalances, the secondary control must modify primary level parameters based on the information exchanged among the μG components through the system communication network [16]. Generally, the implementation of the secondary control strategy can be centralized [9], [17] or distributed [18]–[20]. Centralized techniques, however, provide reduced reliability, since the central controller imposes a single point of

Waner Wodson A. G. da Silva is with the Federal University of Itajuba (UNIFEI), Itabira, Brazil, e-mail: waner@unifei.edu.br.

Thiago R. Oliveira is with Electronic Engineering Department, Federal University of Minas Gerais (UFMG), Belo Horizonte, Brazil, e-mail: troliveira@cpdee.ufmg.br

Pedro F. Donoso-Garcia is with the Electronic Engineering Department, Federal University of Minas Gerais (UFMG), Belo Horizonte, Brazil, e-mail: pedro@cpdee.ufmg.br

This work was supported in part by the Universidade Federal de Itajuba (UNIFEI) and in part by Universidade Federal de Minas Gerias (UFMG).

This article has been accepted for publication in a future issue of this journal, but has not been fully edited. Content may change prior to final publication. Citation information: DOI 10.1109/TPEL.2020.3009619, IEEE Transactions on Power Electronics

failure (SPoF). Therefore, distributed control methods become a more appealing option [17], [18], [21].

Voltage restoration is usually achieved by a voltage-shifting value added to the voltage reference of the converters' voltage control loop. Power sharing correction, on the other hand, can be achieved by (i) droop coefficient adjustment or by (ii) voltage-shifting. The methods based on (i) [11], [16], [22]–[26] modify the droop coefficient in order to compensate for the line impedance influence. However, system dynamics are also affected and hence changes in the droop coefficient should be limited in order to prevent instability. The control techniques based on (ii) [3], [5], [7], [18], [27]–[34] usually rely on two control loops to define the total voltage-shifting term. The first loop is responsible for voltage restoration, whilst the second loop enforces power sharing. In addition, information shared between converters comprises at least of two parameters: the local dc bus voltage and the output current/power.

Another approach is to use only one control loop at the secondary level in order to achieve power sharing and voltage restoration simultaneously. In [35]–[37], the proposed techniques consist of only modifying the droop coefficient to achieve power sharing and, by decreasing its value, the voltage deviation is reduced, but a steady state error will be present in the dc bus voltage. In [20], [38], voltage-shifting is performed based on the average value of the converters' output currents, load sharing is reached and voltage deviation is improved due to the attenuation of the droop effect, however, the average bus voltage is not corrected.

In [2], [39], [40], secondary control strategies for attaining power sharing and voltage restoration are proposed for isolated μGs. In these proposals, each converter conveys information about just one parameter with its neighbors and receives the dc bus voltage informed by a common meter. In spite of good performance, the use of a common measurement introduces a SPoF and reduces reliability and expandability of the μG. In [41], [42], the control technique is also based on only one variable exchanged between converters. In these approaches, the proportional power sharing control is realized through a distributed consensus-based algorithm, whereas voltage restoration is achieved in a decentralized manner, where each converter compensates its own droop voltage. However, as mentioned in [42], a steady state error in the average dc bus voltage will always be present.

The objective of this work is to propose a consensus-based distributed secondary control strategy based on voltage-shifting that is able to attain proportional power sharing and dc bus voltage restoration simultaneously. Unlike previous works, where a set of electrical parameters is exchanged among the converters through the communication network, the proposed technique relies on a single information called the λ factor, which is calculated based on the converters output power and measured dc bus voltage. Periodically, each converter computes its own λ and broadcasts it to neighboring converters through a low bandwidth communication (LBC) link. Locally, a converter employs the received information to determine an average λ and with that the voltage-shifting correction term is generated by means of a simple unity-gain integrator as the secondary layer compensator. It will be shown that as the system gradually reaches consensus, i.e., it converges to an average global λ, proportional power sharing and dc bus voltage restoration are achieved. The total number of neighbors seen by a converter is determined in every control cycle by the number of λ received, thus, the algorithm can deal with dynamic changes in the μG configuration and communication failures, providing plug-and-play capability and flexibility. Moreover, the proposed technique eliminates the necessity for designing and decoupling multiple secondary control loops, employing dc bus voltage observers or common point measurement, while also reducing the information traffic. At last, a comparison of the main features of the proposed technique with other consensus-based algorithms available in literature is provided in Tab. I.

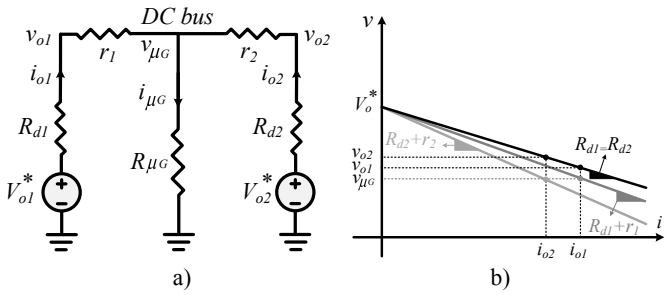

Fig. 2. Simplified model of a dc microgrid.

This paper is outlined as follows: Section II discusses the voltage-shifting influence on power/current sharing and voltage restoration. Section III presents the proposed distributed control technique. Section IV analyzes the system voltage stability. Section V and VI present the simulation and experimental results, respectively, and the paper conclusions are shown in Section VII.

II. Voltage-Shifting Influence on Power Sharing and Voltage Deviation in Droop Controlled μGs

Consider the simplified model of a μG dc bus, presented in Fig. 2.a. It is composed by two converters (*Conv-1* and *Conv-2*), represented by their steady state Thevenin equivalent circuit, where V_{o1}^* and V_{o2}^* are the nominal reference voltages, R_{d1}, R_{d2} are the droop resistances or droop coefficients, v_{o1}, v_{o2}, i_{o1}, i_{o2} are the converters' output voltage and current, respectively, r_1, r_2 are the line resistances, $R_{\mu G}$ is the microgrid load and v_μ is the load voltage. Assuming that the converters are equal, thus, $V_{o1}^* = V_{o2}^* = V_o^*$, $R_{d1} = R_{d2}$ and $r_1 \neq r_2$, Fig. 2.b shows the converters droop characteristic, considering the influence of r_1 and r_2.

Based on Fig. 2.a, it can be defined

$$\begin{aligned} i_{o1} &= \frac{V_{o1}^*(R_{d2}+r_2) + R_{\mu G}(V_{o1}^* - V_{o2}^*)}{\alpha + \beta R_{\mu G}} \\ i_{o2} &= \frac{V_{o2}^*(R_{d1}+r_1) + R_{\mu G}(V_{o2}^* - V_{o1}^*)}{\alpha + \beta R_{\mu G}} \end{aligned} \tag{1}$$

This article has been accepted for publication in a future issue of this journal, but has not been fully edited. Content may change prior to final publication. Citation information: DOI 10.1109/TPEL.2020.3009619, IEEE Transactions on Power Electronics

TABLE I: Main features of consensus-based secondary control algorithms for voltage restaoration and power-sharing.

Literature	Information	Sec. ctrl. loops	Meth.	Comments
[43]	v s u	multiple	vs	utilizes the tertiary control to achieve multiple objectives
[3], [18], [32], [34], [44], [45]	v i	multiple	vs	employs two PI compensators: one to restore the average voltage and other for current sharing
[23]	v i	multiple	da	two PI compensators: one to restore the average voltage and other for droop adjustment
[30]	v,i dV/dt	multiple	vs	three control loops: besides the voltage and current average comtrol loops the third is for sharing the dynamic voltage
[27], [29]	v i	multiple	vs	employs one PI compensator where the input is a sum of the outputs of I compensator for average voltage and P compensator for average current
[41]	i $1/r_{ij}$	single	vs	voltage deviation correction is decentralized. However, prior knowledge of the μG configuration is required. *P&P* is not ensured, since consensus algorithm coefficients are based on the line conductances $1/r_{ij}$
[42]	$power$	multiple	da	voltage deviation correction is decentralized.
Proposed technique	λ	single	vs	employs just one unity-gain integrator, attains power sharing and voltage restoration simultaneously and does not require prior knowledge of the μG configuration.

meth.: correction method, where vs is voltage-shifting and da is droop-adjustment. ***P&P*:** Plug-and-play capability

where

$$\begin{aligned}\alpha &= (R_{d1}+r_1)(R_{d2}+r_2)\\ \beta &= R_{d1}+R_{d2}+r_1+r_2.\end{aligned} \tag{2}$$

Conv-1 and *Conv-2* output voltages are expressed by (3) and the average value between them is defined in (4).

$$\begin{aligned}v_{o1} &= V_{o1}^* - R_{d1}i_{o1}\\ v_{o2} &= V_{o2}^* - R_{d2}i_{o2}\end{aligned} \tag{3}$$

$$v_{oavg} = \frac{v_{o1}+v_{o2}}{2} \tag{4}$$

The voltage deviation can be reduced by a voltage-shifting value (δv_{avg}), which is added to the voltage reference ($V_o^* + \delta v_{avg}$) of each converter, so that $v_{oavg} = V_o^*$. Replacing (1) and (3) in (4), δv_{avg} can be defined as

$$\delta v_{avg} = \frac{2R_{d1}R_{d2} + R_{d1}r_2 + R_{d2}r_1}{2(\beta R_{\mu G} + r_1 r_2) + R_{d1}r_2 + R_{d2}r_1} V_o^*. \tag{5}$$

Considering (1), the output current imbalance can be calculated as follows

$$\Delta i_o = i_{o1} - i_{o2} = ... \\ \frac{2(V_{o1}^* - V_{o2}^*)R_{\mu G} + (R_{d2}+r_2)V_{o1}^* - (R_{d1}+r_1)V_{o2}^*}{\alpha + \beta R_{\mu G}}. \tag{6}$$

It indicates that if appropriate voltage-shifting terms $\delta v_{\Delta i1}$ and $\delta v_{\Delta i2}$ are used to adjust V_{o1}^* and V_{o2}^*, respectively, the current sharing error can be mitigated. Therefore,

$$\begin{aligned}V_{o1}^* &= V_o^* + \delta v_{avg} + \delta v_{\Delta i1}\\ V_{o2}^* &= V_o^* + \delta v_{avg} + \delta v_{\Delta i2}.\end{aligned} \tag{7}$$

However, according to (6), $r_1 < r_2$ implies in $\delta v_{\Delta i1} < \delta v_{\Delta i2}$, thus, $\Delta i_o = 0$ leads to $v_{oavg} \neq V_o^*$. Otherwise, $\delta v_{\Delta i2} > 0$ and $\delta v_{\Delta i1} = -\delta v_{\Delta i2}$, implies in $\Delta i_o \neq 0$ and $v_{oavg} = V_o^*$. It is concluded that $r_1 \neq r_2$ precludes achieving concomitant voltage regulation and balanced output currents.

One can express the converters' output power imbalance as

$$\Delta p_o = p_{o1} - p_{o2} = v_{o1}i_{o1} - v_{o2}i_{o2}. \tag{8}$$

Assuming a condition where $\delta v_{\Delta i1} = -\delta v_{\Delta i2} = \delta v_{\Delta i}$ and replacing (1), (3), (5) and (7) in (8), it is obtained Δp_o as a function of $\delta v_{\Delta i}$:

$$\Delta p_o(\delta v_{\Delta i}) = a(\delta v_{\Delta i})^2 + b(\delta v_{\Delta i}) + c \tag{9}$$

where the coefficients a, b and c are defined in (10) with $R_{tj} = R_{dj} + r_j + 2R_{\mu G}$ for $j = 1, 2$.

The converters output power are $p_{o1} = v_{o1}i_{o1}$ and $p_{o2} = v_{o2}i_{o2}$, so that, $\Delta i_o = 0$ results in $p_{o1} < p_{o2}$. For the condition where $\delta v_{\Delta i1} = -\delta v_{\Delta i2} = \delta v_{\Delta i}$ and $\Delta p_o(\delta v_{\Delta i}) = 0$, it implies in $\Delta v_o i_{o2} = \Delta i_o v_{o1}$, producing $p_{o1} = p_{o2}$, hence, it is possible to achieve simultaneous power sharing and regulated dc bus voltage by using a voltage-shifting term $\delta v_V = \delta v_{avg} \pm \delta v_{\Delta i}$. It is noteworthy that, since line resistances are not compensated, a small error between v_{oavg} and v_μ is expected.

III. Principle of the Proposed Strategy

The proposed technique aims at computing a single voltage-shifting term (δv_V), for each converter, that promotes accurate and proportional power sharing and dc bus voltage restoration. A LBC network is used to exchange information between neighboring converters and a consensus-based algorithm is employed to converge the information state to an average value. However, unlike previous proposals, where multiple converter measurements are exchanged in the LBC link and multiple control loops are required to compose the proper δv_V, the technique proposed herein defines a factor (λ) as the information state instead, which is computed locally by each

This article has been accepted for publication in a future issue of this journal, but has not been fully edited. Content may change prior to final publication. Citation information: DOI 10.1109/TPEL.2020.3009619, IEEE Transactions on Power Electronics

$$a = \frac{R_{d2}R_{t1}^2 - R_{d1}R_{t2}^2 + (\alpha + \beta R_{\mu G})(R_{d2} - R_{d1} + r_2 - r_1)}{(\alpha + \beta R_{\mu G})^2}$$

$$b = V_o^* \left(\frac{(R_{d2} + r_2)(2R_{d1}R_{t2} - \alpha - \beta R_{\mu G}) - (R_{d1} + r_1)(\alpha + \beta R_{\mu G} - 2R_{d2}R_{t1}) - (\beta + 4R_{\mu G})(\alpha + \beta R_{\mu G})}{(\alpha + \beta R_{\mu G})^2} \right) \quad (10)$$

$$c = V_o^{*2} \frac{(\alpha + \beta R_{\mu G})(R_{d2} - R_{d1} + r_2 - r_1) + R_{d2}(R_{d1} + r_1)^2 - R_{d1}(R_{d2} + r_2)^2}{(\alpha + \beta R_{\mu G})^2}$$

converter, according to (11), where v_{oj} is the j-th converter output voltage and $\overline{P}_{oj}$ is a power quantity defined as (12), where p_{oj} is the converter output power, and P_{jmax} is its rated power. The gain $1/2$ is needed to avoid a division by zero in the local controller when $p_{oj} = P_{jmax}$.

$$\lambda_j = \overline{P}_{oj} v_{oj} \quad (11)$$

$$\overline{P}_{oj} = 1 - \frac{1}{2}\frac{p_{oj}}{P_{jmax}} \quad (12)$$

During a control cycle, each converter sends its λ factor to its N neighbors and receives their respective λ factors, through the LBC network. Afterwards, it locally computes a voltage-shifting term as

$$\delta v_{Vj} = \int \left(V_o^* - \frac{\lambda_{avg}}{\overline{P}_{oj}} \right) dt \quad (13)$$

where, V_o^* is the dc bus voltage reference and λ_{avg} is the average λ, defined as

$$\lambda_{avg} = \frac{\lambda_1 + \lambda_2 + \cdots + \lambda_N}{N} \quad (14)$$

In order to deal with communication failures and the addition/removal of new agents, the algorithm defines N as the number of neighboring converters that send information to the j-th converter in a control cycle. The proposed local controller diagram is shown in Fig. 3, where C_v and C_i are the voltage and current loop PI (proportional-integral) compensators, respectively, R_{dj} is the droop coefficient and lowpass filters were used to smooth the output current and power measurements. Assuming, for the sake of argument, that the secondary control strategy is able to converge, then $V_o^* = \frac{\lambda_{avg}}{\overline{P}_{o1}} = \frac{\lambda_{avg}}{\overline{P}_{oN}}$, through (11), (12) and (14) it can be shown that a convergence of δv_V will lead to

$$\frac{p_{o1}}{P_{1max}} = \frac{p_{o2}}{P_{2max}} = \cdots = \frac{p_{oN}}{P_{Nmax}}$$
$$V_o^* = \frac{v_{o1} + v_{o2} + \cdots + v_{oN}}{N} \quad (15)$$

Although there is a single secondary control loop, power sharing and voltage restoration exhibit different time constants. The convergence analysis of each control objective will be addressed separately in the following subsections.

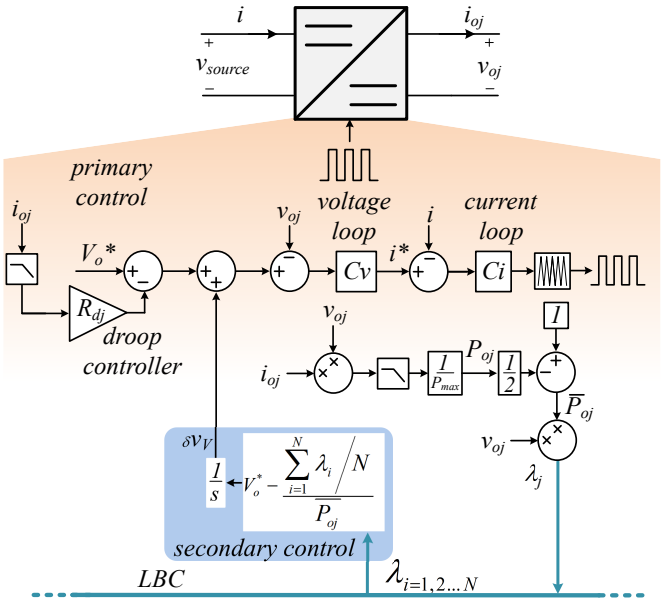

Fig. 3. Diagram of the proposed control.

A. Power sharing convergence analysis

Assuming that the control cycle, i.e., the sampling time of the secondary control layer ($t_{\delta v_V}$), is much greater than the primary control bandwidth, the dynamic behavior of the proposed strategy can be studied considering the simplified μG model of Fig. 2.a. Applying (13) to V_{o1}^* and V_{o2}^* results in a set of nonlinear differential equations, with no explicit analytical solution, thus, the system response can only be assessed by numerical analysis. Evaluating several scenarios with the aid of numerical simulations, it was observed that the power imbalance behavior exhibits a second order system response, which is influenced by the load, droop and line resistances and $t_{\delta v_V}$ as well. Interestingly, when the converters comply with $R_{d1}P_{1max} = R_{d2}P_{2max}$, two different scenarios will exhibit the same dependency on the normalized load power and $t_{\delta v_V}$ if both also exhibit the same load type (resistive or constant power load (CPL)) and the same k_β, where

$$k_\beta = \frac{R_{d1} + R_{d2} + r_1 + r_2}{R_{d1} + R_{d2}} \quad (16)$$

Therefore, the performance of multiple scenarios can be studied by evaluating how changes in k_β impact the system behavior. Notice that the greater the k_β, the more significant

This article has been accepted for publication in a future issue of this journal, but has not been fully edited. Content may change prior to final publication. Citation information: DOI 10.1109/TPEL.2020.3009619, IEEE Transactions on Power Electronics

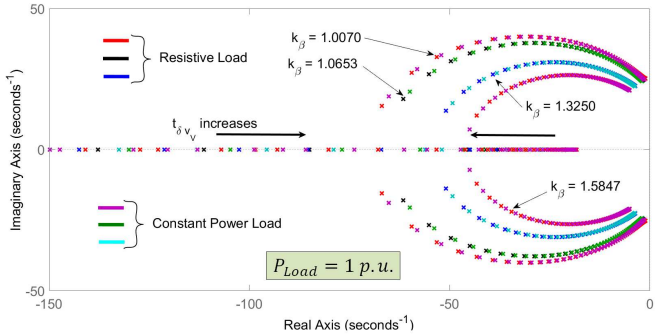

(a) Influence of $t_{\delta v_V}$ on root *loci*.

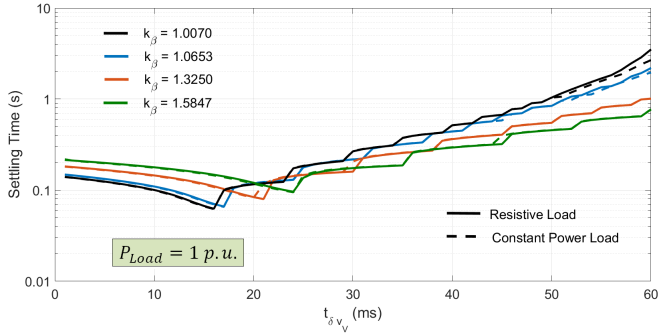

(b) Influence of $t_{\delta v_V}$ on Settling time.

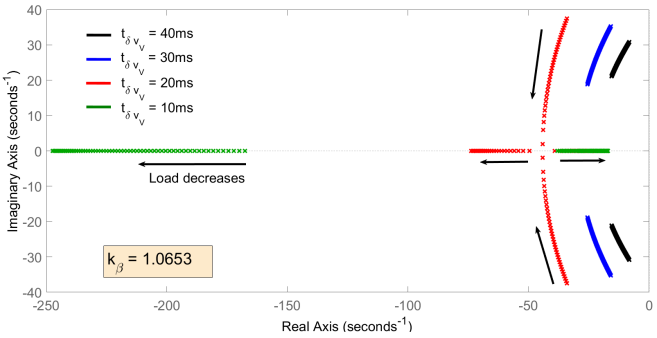

(c) Influence of the load on the root *loci*.

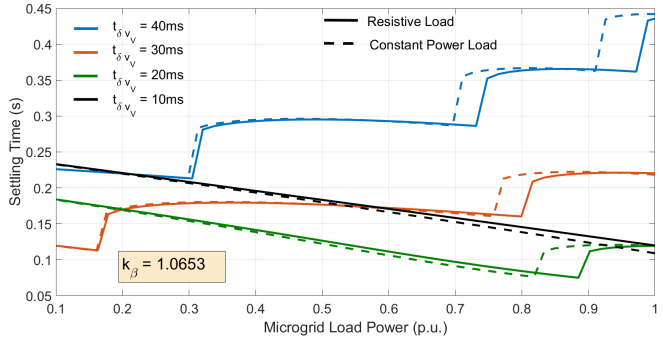

(d) Influence of the load on the Settling Time.

Fig. 4. Assessment of the power sharing behavior. In (a) and (b), $t_{\delta v_V}$ varies from 1 ms to 60 ms. In (c) and (d), P_{Load} varies from 1 p.u. to 0.1 p.u.

are the line resistances in relation to the virtual droop resistances. In order to quantify the system performance in each scenario, a process estimation function was used to estimate a second order system model from the numerical simulation data. Fig. 4 presents the root *loci* and settling time response of the estimated second order model against $t_{\delta v_V}$ and the load power for a μG with resistive load and CPL as well.

It can be noticed that, for very low $t_{\delta v_V}$, the system shows a dominant pole that will grant it a first order behavior. As $t_{\delta v_V}$ increases, system damping is decreased, reducing the power sharing settling time (Δt_{ps}), but as the poles become complex and move towards the RHS of the s-plane, Δt_{ps} also increases. Eventually, for large $t_{\delta v_V}$, the system becomes unstable, e.g., for $k_\beta \approx 1$, critical stability is reached at $t_{\delta v_V} \approx 65ms$. An increase in k_β as well as a decrease in the load power raises system damping, reducing Δt_{ps} for complex poles and the contrary for real poles. It is also noticed that in the load variation range, Δt_{ps} varied roughly 6dB, whereas in the $t_{\delta v_V}$ range, it varied up to 35dB, hence, proper selection of $t_{\delta v_V}$ is crucial for the successful operation of the μG. It is noteworthy that, although small differences can be observed between the resistive and CPL behaviors, both types performed similarly. Since the proposed strategy does not alter the output impedance of the converters, once the primary level is designed to ensure a stable operation in the presence of CPL, the secondary layer will not degenerate the load dynamics.

B. Average voltage convergence analysis

Once power balancing is achieved, the secondary-layer control feedback will become

$$\frac{\overline{P}_o v_{o1} + \overline{P}_o v_{o2}}{2\overline{P}_o} = \frac{v_{o1} + v_{o2}}{2} = v_{oavg}. \tag{17}$$

Consequently, the secondary control law can be rewritten as

$$\delta v_{Vj}(t) \approx \int \left(V_o^* - v_{oavg}(t)\right) dt \tag{18}$$

Assuming that Δt_{ps} is negligible in relation to the voltage restoration response, replacing (18) in (1)-(4), yields

$$\begin{aligned} v_{oavg}(t) &= V_o^* \left(1 - k_{vo}\right) e^{-(1-k_{vo})t} \\ k_{vo} &= \frac{R_{d1}(R_{d2} + r_2) + R_{d2}(R_{d1} + r_1)}{2(\alpha + \beta R_{\mu G})} \end{aligned} \tag{19}$$

Therefore, the dc bus voltage restoration will show a first order response with a time constant $\tau_v = (1 - k_{vo})^{-1}$. Obviously, $\Delta t_{ps} << \tau_v$ is required. Fig. 5 illustrates the transient response of the proposed technique, for a simplified dc μG model with the parameters given in Tab. II and $R_{\mu G} = 40\Omega$, which leads to a $\tau_v \approx 1s$ and $\Delta t_{ps} \approx 0.176s$.

It can be seen that before the secondary control strategy is enabled, the μG operates with $v_{oavg} \approx 370V$, a load voltage of 369V and a power mismatch of 0.13 p.u. In $t = 0.5s$ the secondary control is activated. It can be noticed that at first, the voltage-shifting terms δv_{V1} and δv_{V2} are predominantly

This article has been accepted for publication in a future issue of this journal, but has not been fully edited. Content may change prior to final publication. Citation information: DOI 10.1109/TPEL.2020.3009619, IEEE Transactions on Power Electronics

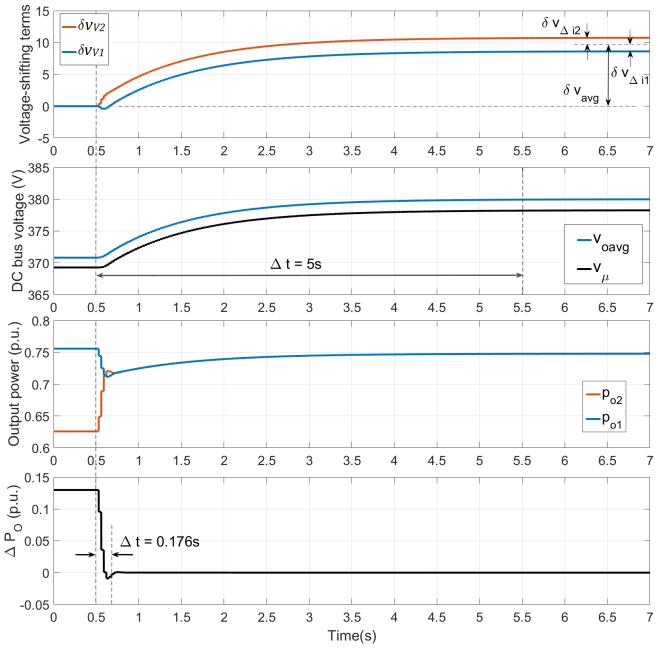

Fig. 5. Evolution of δv_V and its effect on bus voltage and power imbalance.

defined by $\delta v_{\Delta i}$, hence they diverge from each other, forcing the output power imbalance to be mitigated in $\Delta t_{ps} = 0.176s$. Once $p_{o1} = p_{o2}$, the argument of the secondary control integral action of both converters is the same, therefore the voltage-shifting terms evolve defining a δv_{avg} that leads the dc bus voltage to converge to $v_{oavg} = 380V$ in $\Delta t = 5\tau_v \approx 5s$. In steady state, $\delta v_{\Delta i2} = -\delta v_{\Delta i1} = 1.035V$ and $\delta v_{avg} = 9.665V$.

Since the electrical and communication systems interact with each other, they are affected by the transmission rate and communication network configuration [3]. Therefore, it is important to consider the discrete nature of the communication network, hence the secondary layer integral controller is implemented in discrete time, where the time interval between control cycles ($t_{\delta v_V}$) should be enough for all converters to send and receive the λ factors and update δv_V.

IV. Stability Analysis

From the μG model in Fig.2, the relationship between the output voltage and current of *Conv-1* can be expressed as:

$$i_{o1} = \gamma v_{o1} - \kappa v_{o2} \tag{20}$$

where

$$\begin{aligned} \gamma &= \frac{r_2 + R_\mu}{r_1 r_2 + r_1 R_{\mu G} + r_2 R_{\mu G}} \\ \kappa &= \frac{R_{\mu G}}{r_1 r_2 + r_1 R_{\mu G} + r_2 R_{\mu G}} \end{aligned} \tag{21}$$

Replacing $\delta v_{avg} + \delta v_{\Delta i}$ for δv_{V1} in (7) and in (3) yields

$$v_{o1} = V_o^* + \delta v_{V1} - R_{d1} i_{o1} \tag{22}$$

Considering (13) and (20)-(22), the closed-loop control diagram of *Conv-1* is shown in Fig. 6. Assuming that $t_{\delta v_V}$ is much

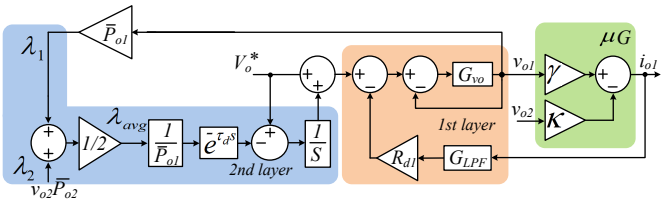

Fig. 6. Closed-loop control diagram for stability analysis.

larger than the converter local control response time, then the converter could be represented by its Thevenin equivalent circuit. The communication delay is represented by $e^{-\tau_d s}$ and the closed-loop transfer function is expressed as [5], [7]:

$$G_{vo} = \frac{G_{PI} G_C}{1 + G_{PI} G_C} \tag{23}$$

where G_{PI} and G_C are the voltage loop PI compensator and the current loop transfer function, respectively. G_C can be represented as a delay unit [7]. Therefore, from Fig. 6, *Conv-1* output voltage is expressed as:

$$v_{o1} = \frac{\left[V_o^*(1 + 1/s) + v_{o2}(\kappa R_{d1} G_{LPF} - \frac{e^{-\tau_d s}\overline{P}_{o2}}{2\overline{P}_{o1} s})\right] G_{vo}}{1 + (\gamma R_{d1} G_{LPF} + \frac{e^{-\tau_d s}}{2s}) G_{vo}} \tag{24}$$

where $G_{LPF} = \frac{2\pi f c}{s + 2\pi f c}$.

In order to assess the stability analysis model accuracy, Fig. 7 shows the simulated behavior of *Conv-1* and *Conv-2* in different operating conditions for both the evaluated model and the complete converter switching model, considering the parameters described in Tab. II. At t = 0.1s (A) the proposed technique was enabled and at t = 0.5s (B), $R\mu G$ was reduced to 40Ω and, finally, at $t = 0.8$s (c), r_1 changes to 0.4 Ω. It is observed that the models hold a high correlation.

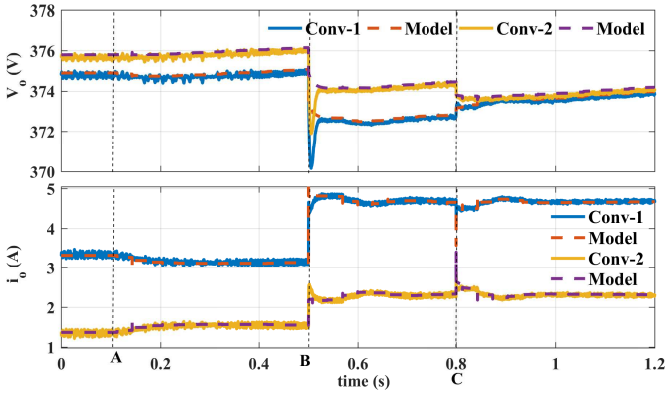

Fig. 7. Output voltage and current behavior of the switched and stability analysis models of a μG.

Applying a small-signal linearization on the variables in (24), the small signal model, thus, can be represented as:

$$\left.\frac{\hat{v}_{o1}}{\hat{V}_o^*}\right|_{\hat{v}_{o2}=0} = \frac{V_o^*(1 + 1/s) G_{vo}}{1 + (\gamma R_{d1} G_{LPF} + \frac{e^{-\tau_d s}}{2s}) G_{vo}} \tag{25}$$

The dominant poles root *loci* under variations on r_1, R_{d1}, $R_{\mu G}$ and τ_d are shown in Fig. 8, also for the parameters

This article has been accepted for publication in a future issue of this journal, but has not been fully edited. Content may change prior to final publication. Citation information: DOI 10.1109/TPEL.2020.3009619, IEEE Transactions on Power Electronics

described in Tab. II. To verify the influence of line impedance on the closed-loop system poles, r_1 varies from 0.05Ω to 1Ω and r_2 is fixed. R_{d1} varies from $0.5R_{d1}$ to $2R_{d1}$ with R_{d2} fixed and $R_{\mu G}$ is varied from $0.5R_{\mu G}$ to $1000R_{\mu G}$, which allows to evaluate the conditions from heavy μG load up to light load. The effect of λ_{avg} calculation delay (τ_d) was assessed considering $t_{\delta v_V}$ as a reference, therefore, τ_d was varied from $1ms$ to $100ms$. In all four analyzes, the poles *loci* were affected, however, in the considered variation ranges no small-signal instability is foreseen. It is noticed, as it is the case for consensus-based algorithms, that time delay produces complex poles and its increase shifts them towards the RHS of the s-plane, reducing damping, as also discussed in [42].

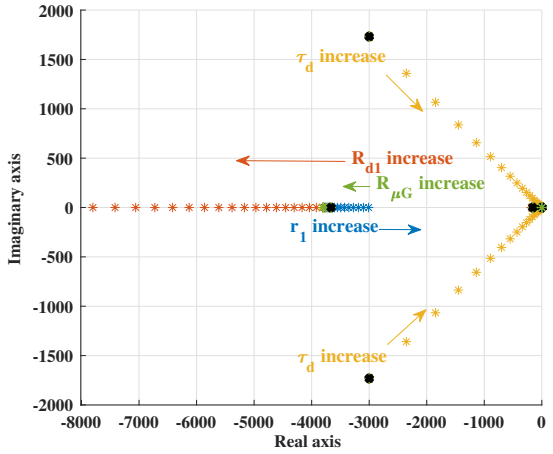

Fig. 8. Stability analysis of the converters.

A. Stability Analysis Generalized for N converters

Assuming the circuit of Fig. 2.a, now with N converters on the dc-bus, then the output current in each converter can be

TABLE II: STABILITY ANALYSIS PARAMETERS

Item	Symbol	Value
Nominal voltage	V_o^*	$380V$
Line impedance	$r_{1,2}$	0.1, 0.9Ω
Droop Coefficient	$R_{d1,2}$	1.54, 3.08Ω
Load resistance	$R_{\mu G}$	80Ω
Integrator time interval	$t_{\delta v_V}$	$30ms$
Calculation delay	τ_d	$1...100ms$
LPF cut-off frequency	f_c	$1.5kHz$

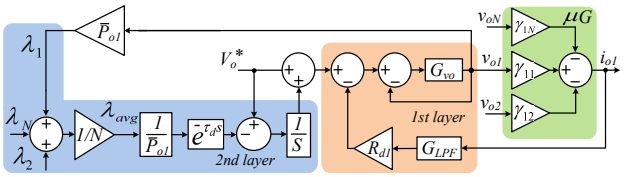

Fig. 9. Control diagram for stability analysis for N converters.

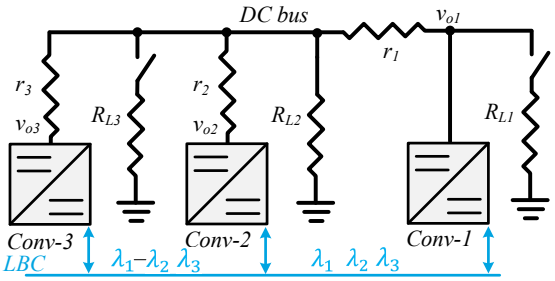

Fig. 10. Simulated DC microgrid.

calculated in matrix form:

$$[R]\,[i_o] = [v_o] \rightarrow \begin{bmatrix} R_{\mu G}+r_1 & R_{\mu G} & \dots & R_{\mu G} \\ R_{\mu G} & R_{\mu G}+r_2 & \dots & R_{\mu G} \\ \vdots & \vdots & \vdots & \vdots \\ R_{\mu G} & R_{\mu G} & \dots & R_{\mu G}+r_N \end{bmatrix} \begin{bmatrix} i_{o1} \\ i_{o2} \\ \vdots \\ i_{oN} \end{bmatrix} = \begin{bmatrix} v_{o1} \\ v_{o2} \\ \vdots \\ v_{oN} \end{bmatrix} \quad (26)$$

The closed-loop control diagram of *Conv-1* with N converters can be represented by Fig. 9, where $\gamma_{j,k}$ is an element of matrix $[\gamma]$ and $[\gamma] = [R]^{-1}$. Considering (25), γ becomes $\gamma_{1,1}$, hence, it is concluded that the effect of adding/removing converters on stability is similar to the effect of R_{d1} variation.

V. Simulation Results

In order to evaluate the proposed method, a computational simulation of a dc microgrid with three Dual Active Bridge (DAB) converters, as depicted in Fig. 10, was performed using PLECS. The simulation parameters are described in Table III.

The simulation study conducted in this section assumed the following initial conditions: $v_{oavg} = 376.2V$, $p_{o1} = 0.43p.u.$, $p_{o2} = 0.41p.u.$, p_{o3} = $0.31p.u.$ and with load R_{L1} connected to the dc bus. At first, the dynamic behavior of the proposed method in achieving proportional power sharing and restoring the dc bus voltage under load variations was evaluated and compiled in the results shown in Fig. 11. At $t = 1s$ (event A), the secondary layer control is enabled, starting the power sharing and voltage restoration processes. It can be observed that proportional power sharing is achieved after $\Delta t \approx 295ms$, resulting in $p_{o1} = p_{o2} = p_{o3} = 0.41p.u.$, leading to steady state ouput currents of $i_{o1} = 2.46A$, $i_{o2} = 1.25A$ and $i_{o3} = 1.27A$. As mentioned in Section II, accurate proportional current sharing is not attained, i.e., $0.5i_{o1} \neq i_{o2}$ and $i_{o2} \neq i_{o3}$, however the current imbalance is reduced, e.g., Δi_{o23} decreases from $0.49A$ (initial condition) to $0.02A$.

This article has been accepted for publication in a future issue of this journal, but has not been fully edited. Content may change prior to final publication. Citation information: DOI 10.1109/TPEL.2020.3009619, IEEE Transactions on Power Electronics

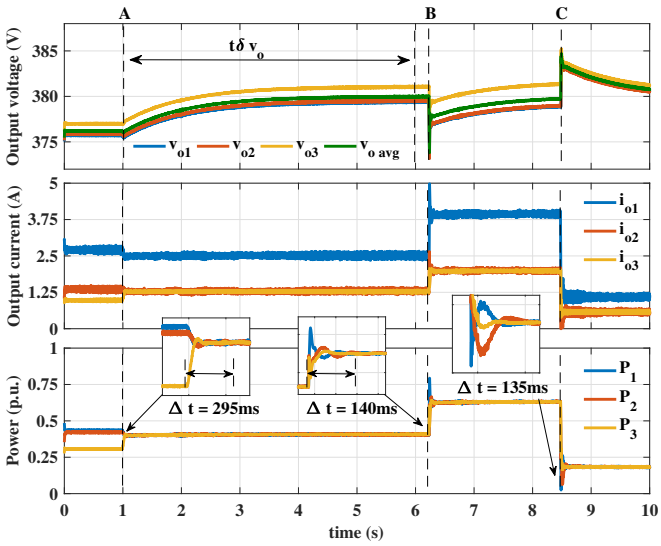

Fig. 11. Simulated secondary control behavior under load disturbances.

The dc bus voltage is regulated to 380V after $t_{\delta v_o} \approx 5s$, as previously predicted. At $t = 6.2s$ (B), the load resistance R_{L3} is connected to the dc bus, promoting a voltage sag of about 2V and power imbalance between converters. The secondary control is able to once again achieve proportional power sharing after $\Delta t = 140ms$, converging to $p_{o1} = p_{o2} = p_{o3} = 0.63\ p.u.$ and the dc bus voltage is gradually regulated. At $t = 8.5s$ (C), both loads R_{L1} and R_{L3} are disconnected simultaneous from dc bus, elevating the dc bus voltage about 2V. It can be seen that after $\Delta t = 135ms$, proportional power sharing was attained with $p_{o1} = p_{o2} = p_{o3} = 0.18p.u.$ As predicted in Section III, since the net load power variation in (B) and (C) is lower than in (A), the power sharing settling time in these two events were smaller than in the first one, also slight variations in damping can be perceived what was also expected, since load switching changes the equivalent line resistances between converters, altering k_β. Moreover, load variations had negligible effect on voltage restoration dynamic.

TABLE III: SIMULATION PARAMETERS

Item	Symbol	Value
Nominal Voltage	V_O^*	$380V$
Line impedance	$r_{1,2,3}$	0.1, 0.1, 0.9Ω
Droop Coefficient	$R_{d1,2,3}$	1.54, 3.08, 3.08Ω
Power ratio	$P_{1,2,3}$	3.2, 1.6, $1.6kW$
Load	$R_{L1,L2,L3}$	133, 170, 133Ω
Integrator time interval	$t_{\delta v_V}$	$30ms$
Switching frequency	f_{sw}	$15kHz$
DAB transformer	n	7.9 : 1
PI voltage controller	PI	$k_p = 1.8, k_i = 276$
PI current controller	PI	$k_p = 0.3, k_i = 20$
Current and voltage sensor gains	$H_{i,v}$	0.1, 0.01
LPF cut-off frequency	f_c	$1.5kHz$

Afterwards, the plug-and-play capability of the proposed algorithm and its response to communication failures were evaluated. Fig 12 shows the continuation of the simulation study started in Fig. 11, where at $t = 12.5s$ (D), *Conv-2* is disconnected from the microgrid dc bus. As a result, the dc bus voltage drops about $1V$ and a new power sharing configuration is achieved, where *Conv-1* and *Conv-3* assume the extra load and reach $p_{o1} = p_{o3} = 0.245p.u.$ In $t = 15s$ (E), R_{L1} is reconnected to the dc bus, which disturbs the dc bus voltage and increases the μG power demand. The results show that the strategy was able to supply the extra power with proportional power sharing and correct the dc bus voltage deviation. In $t = 19.5s$, *Conv-2* is reconnected to the dc bus. It can be observed that just after reconnection, the strategy attains a new power sharing configuration. It can be noticed that during the disconnection and reconnection of one converter, the secondary control was able to sustain accurate proportional power sharing and voltage restoration with similar characteristics.

A communication failure in *Conv-1* occurs at $t = 22s$ (G), leaving it to operate isolated from the others. The secondary control still regulates the average bus voltage and enforces proportional power sharing between *Conv-2* and *Conv-3*, leading to $p_{o2} = p_{o3} = 0.39p.u.$, with a $\Delta i_{o23} = 0.03A$, however, since *Conv-1* only operates with droop control, the average dc bus voltage among all three converters becomes $v_{oavg} = 379.7V$. At $t = 24.5s$, R_{L3} is connected to the dc bus disturbing the system voltage and power sharing. Since the control action tends to regulate the average dc bus voltage between *Conv-2* and *Conv-3*, those converters assume a greater share of the load power, whereas *Conv-1* senses an increase in the bus voltage and reduces its output power, hence power sharing is no longer proportional among all converters. It is interesting to notice that although the isolation of one converter precludes accurate power sharing and voltage restoration to be achieved, it does not prevent the μG to maintain operation. In $t = 27.5s$ (I), the communication with *Conv-1* is restored and so the proportional power sharing.

VI. Experimental Results

The proposed control technique has been implemented in a reduced scale dc microgrid workbench, as presented in Fig. 13. *Conv-1* is a $3.2kW$ two-stage bidirectional utility interface converter, where the dc-dc stage realizes a primary level droop control and the proposed secondary level strategy, whereas the ac-dc stage regulates the internal dc link in 550V. Since the converter local control has no influence on the proposed strategy, the primary level control diagram is omitted here. *Conv-2* and *Conv-3* are $1.6kW$ DAB converters that interface the dc bus and battery banks. The primary and secondary control layers of each converter were implemented in a TMS320F28335 DSP and the *LBC* network was developed using CAN 2.0 with $125kbps$. The converter parameters are the ones described in Table III.

Fig. 14 shows the results of the proposed control for some load conditions. The μG initially ($t < 1s$) operates with

This article has been accepted for publication in a future issue of this journal, but has not been fully edited. Content may change prior to final publication. Citation information: DOI 10.1109/TPEL.2020.3009619, IEEE Transactions on Power Electronics

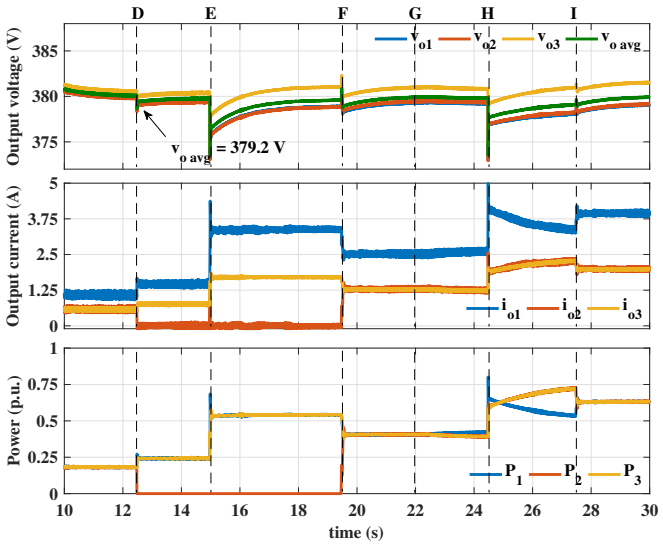

Fig. 12. Secondary control behavior under converter disconnection/reconnection and communication failure.

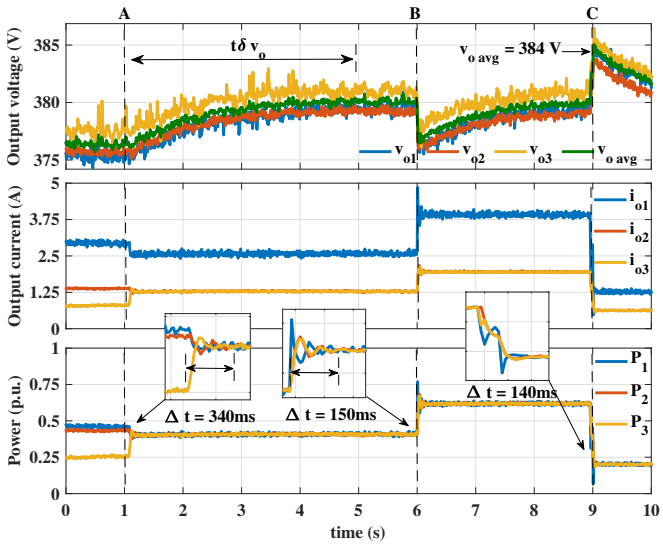

Fig. 14. Experimental results for control initialization and load disturbaces.

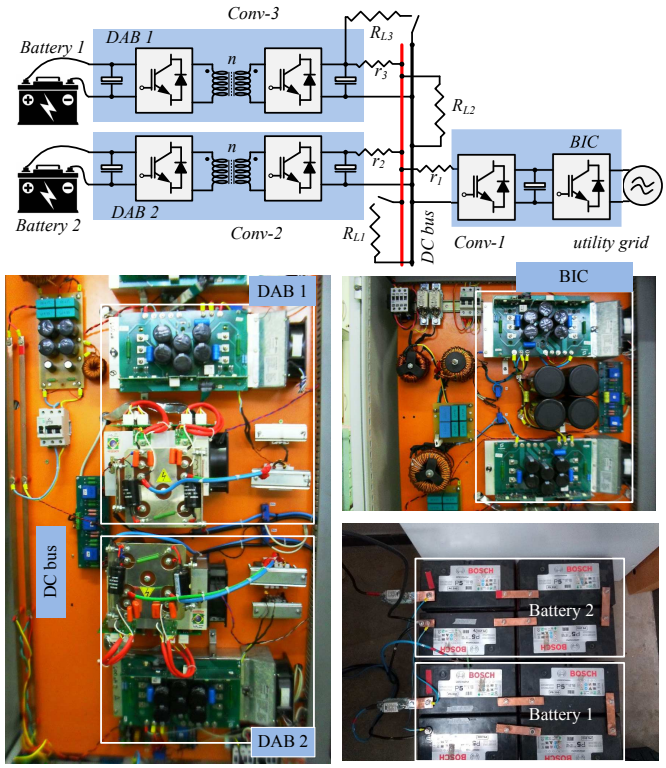

Fig. 13. DC microgrid experimental setup.

$v_{oavg} = 375.4V$, $p_{o1} = 0.47$, $p_{o2} = 0.44$ and $p_{o3} = 0.26p.u.$, $\Delta i_{o23} = 0.61A$ and with R_{L1} connected to the dc bus. At $t = 1s$ (A), the secondary control layer is enabled, it is observed that power sharing correction takes $\Delta t = 340ms$ and the output powers attain $0.40p.u.$. The average dc bus voltage converges to $380V$ in $t_{\delta v_o} \approx 4.5s$. At $t = 6s$ (B), R_{L3} is connected to the dc bus producing a voltage drop of 3.6V and disturbing the μG power sharing, which takes about $\Delta t = 150ms$ to be corrected. At $t = 9s$ (C), R_{L1} and R_{L3} are simultaneously disconnected from the microgrid, generating an average voltage elevation of $4V$. Power sharing is achieved in $\Delta t \approx 140ms$. As it can be observed, the power sharing settling time is approximately the same for load connection and disconnection.

Fig. 15 shows the control performance when submitted to a converter connection/disconnection and communication failure. The results were collected right after the ending of Fig. 14. At $t = 11.5s$ (D), *Conv-2* is disconnected from the dc bus, imposing a small voltage drop of $0.5V$, the remaining converters proportionally assume the load power. At $t = 15.5s$ (E), R_{L1} is connected to the dc bus and the converters output power are corrected to $0.56p.u.$ with the following output currents $i_{o1} = 3.46$ A and $_{io3} = 1.69A$. In $t = 18.4s$ (F), *Conv-2* is reconnected to the dc bus and immediately participates in power sharing which is corrected in $\Delta t = 200ms$. In $t = 21s$ (G), a communication failure occurs, leaving *Conv-1* isolated from the others. Since dc bus voltage deviation correction is still being performed, the output power of *Conv-2* and *Conv-3* are increased, whereas *Conv-1*, due to the droop effect, reduces its output power, hence p_{o1} becomes smaller than p_{o2} and p_{o3}. R_{L3} is connected to the dc bus at $t = 22.7s$ (H), increasing the power sharing imbalance of *Conv-1* in relation to *Conv-2* and *Conv-3*, Finally, at $t = 26.1s$ (I) the communication with *Conv-1* is reestablished and the control converges to $v_{oavg} = 380V$ with $p_{o1} = p_{o2} = p_{o3} = 0.61p.u.$.

VII. Conclusion

This paper proposed a dc microgrid distributed secondary layer control strategy based on voltage-shifting that is able to accomplish accurate and proportional power sharing and voltage restoration simultaneously. The strategy defines a λ factor, which carries information concerning the converter output voltage and power as the consensus information state to

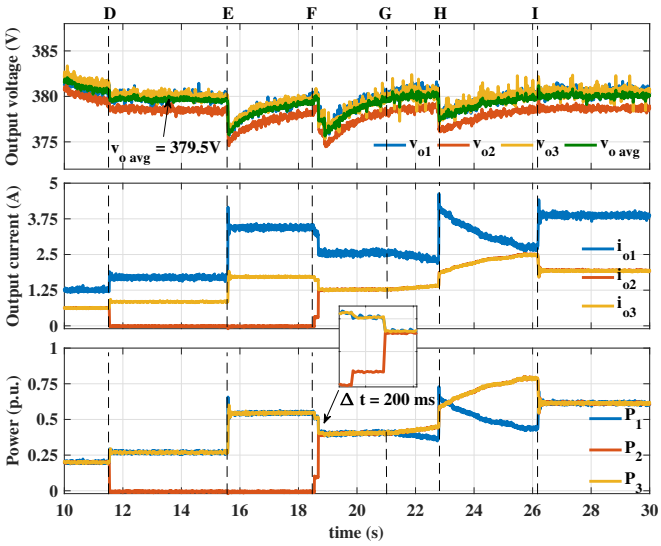

Fig. 15. Experimental results with load perturbation and failure.

be shared between converters through a low-bandwidth communication (LBC) network. Therefore, just one information per converter is broadcasted, simplifing the secondary control architecture and also reducing the required information traffic. Each converter computes the average λ using the information received from the LBC link, and through a simple secondary layer controller composed of a unity-gain integrator generates a voltage-shifting term that adjusts its output voltage reference. The behavior of the proposed technique was assessed through simulation and experimental results, which have shown that both control objectives are achieved under distinct operation conditions, it also provides *plug-and-play* capability to the microgrid, since the connection/disconnection of a converter is quickly compensated by the secondary control. The results have shown as well that in case of a communication failure that isolates one of the converters, the strategy will maintain power sharing and voltage deviation correction between the converters still connected to the LBC link, thus, a small average dc bus voltage error and power imbalance between the isolated converter and the rest are expected, however, the system can still sustain the operation, which provides great reliability. Moreover, the proposed strategy presented a stable behavior over different parameters variation and the inaccuracies in the voltage and current measurements did not compromise the voltage regulation performance. Therefore, the proposed control presents itself as a robust strategy for power sharing and voltage restoration under various operating conditions.

ACKNOWLEDGEMENT

The authors would like to thank PRPq/UFMG by the financial support given to this project through the Programa Institucional de Taxa de publicação em periódicos indexados and to thank PRPPG/UNIFEI by the financial support to publication to this work through the Edital 01/2020 - Apoio à Comunicação Científica.

REFERENCES

[1] J. M. Guerrero, J. C. Vasquez, J. Matas, M. Castilla, and L. G. de Vicuna, "Control strategy for flexible microgrid based on parallel line-interactive ups systems," *IEEE Transactions on Industrial Electronics*, vol. 56, no. 3, pp. 726–736, March 2009.

[2] F. Guo, Q. Xu, C. Wen, L. Wang, and P. Wang, "Distributed secondary control for power allocation and voltage restoration in islanded dc microgrids," *IEEE Transactions on Sustainable Energy*, vol. 9, no. 4, pp. 1857–1869, Oct 2018.

[3] L. Meng, T. Dragicevic, J. Roldán-Pérez, J. C. Vasquez, and J. M. Guerrero, "Modeling and sensitivity study of consensus algorithm-based distributed hierarchical control for dc microgrids," *IEEE Transactions on Smart Grid*, vol. 7, no. 3, pp. 1504–1515, May 2016.

[4] P. Ghalebani and M. Niasati, "A distributed control strategy based on droop control and low-bandwidth communication in dc microgrids with increased accuracy of load sharing," *Sustainable Cities and Society*, vol. 40, pp. 155–164, 2018. [Online]. Available: http://www.sciencedirect.com/science/article/pii/S221067071731627X

[5] K. D. Hoang and H. Lee, "Accurate power sharing with balanced battery state of charge in distributed dc microgrid," *IEEE Transactions on Industrial Electronics*, vol. 66, no. 3, pp. 1883–1893, March 2019.

[6] S. Augustine, M. K. Mishra, and N. Lakshminarasamma, "Adaptive droop control strategy for load sharing and circulating current minimization in low-voltage standalone dc microgrid," *IEEE Transactions on Sustainable Energy*, vol. 6, no. 1, pp. 132–141, Jan 2015.

[7] X. Lu, J. M. Guerrero, K. Sun, and J. C. Vasquez, "An improved droop control method for dc microgrids based on low bandwidth communication with dc bus voltage restoration and enhanced current sharing accuracy," *IEEE Transactions on Power Electronics*, vol. 29, no. 4, pp. 1800–1812, April 2014.

[8] A. Chen, D. Xie, S. Yu, C. Gu, and Y. Li, "Comprehensive evaluation index based on droop control for dc distribution system dispatching," *International Journal of Electrical Power & Energy Systems*, vol. 106, pp. 528 – 537, 2019. [Online]. Available: http://www.sciencedirect.com/science/article/pii/S0142061518316314

[9] T. Dragičević, J. M. Guerrero, J. C. Vasquez, and D. Škrlec, "Supervisory control of an adaptive-droop regulated dc microgrid with battery management capability," *IEEE Transactions on Power Electronics*, vol. 29, no. 2, pp. 695–706, Feb 2014.

[10] L. Meng, T. Dragicevic, J. M. Guerrero, and J. C. Vasquez, "Dynamic consensus algorithm based distributed global efficiency optimization of a droop controlled dc microgrid," in *2014 IEEE International Energy Conference (ENERGYCON)*, May 2014, pp. 1276–1283.

[11] P. Wang, X. Lu, X. Yang, W. Wang, and D. Xu, "An improved distributed secondary control method for dc microgrids with enhanced dynamic current sharing performance," *IEEE Transactions on Power Electronics*, vol. 31, no. 9, pp. 6658–6673, Sep. 2016.

[12] Q. Shafiee, J. M. Guerrero, and J. C. Vasquez, "Distributed secondary control for islanded microgrids—a novel approach," *IEEE Transactions on Power Electronics*, vol. 29, no. 2, pp. 1018–1031, Feb 2014.

[13] J. Fang, Z. Shuai, X. Zhang, X. Shen, and Z. J. Shen, "Secondary power sharing regulation strategy for a dc microgrid via maximum loading factor," *IEEE Transactions on Power Electronics*, pp. 1–1, 2019.

[14] X. Lu, J. M. Guerrero, K. Sun, J. C. Vasquez, R. Teodorescu, and L. Huang, "Hierarchical control of parallel ac-dc converter interfaces for hybrid microgrids," *IEEE Transactions on Smart Grid*, vol. 5, no. 2, pp. 683–692, March 2014.

[15] C. Jin, J. Wang, and P. Wang, "Coordinated secondary control for autonomous hybrid three-port ac/dc/ds microgrid," *CSEE Journal of Power and Energy Systems*, vol. 4, no. 1, pp. 1–10, March 2018.

[16] G. Lee, B. Ko, J. Cho, and R. Kim, "A distributed control method based on a voltage sensitivity matrix in dc microgrids with low-speed communication," *IEEE Transactions on Smart Grid*, pp. 1–1, 2018.

[17] J. M. Guerrero, J. C. Vasquez, J. Matas, L. G. de Vicuna, and M. Castilla, "Hierarchical control of droop-controlled ac and dc microgrids—a general approach toward standardization," *IEEE Transactions on Industrial Electronics*, vol. 58, no. 1, pp. 158–172, Jan 2011.

[18] V. Nasirian, S. Moayedi, A. Davoudi, and F. L. Lewis, "Distributed cooperative control of dc microgrids," *IEEE Transactions on Power Electronics*, vol. 30, no. 4, pp. 2288–2303, April 2015.

[19] T. Dragičević, J. M. Guerrero, and J. C. Vasquez, "A distributed control strategy for coordination of an autonomous lvdc microgrid based on power-line signaling," *IEEE Transactions on Industrial Electronics*, vol. 61, no. 7, pp. 3313–3326, July 2014.

[20] S. Anand, B. G. Fernandes, and J. Guerrero, "Distributed control to ensure proportional load sharing and improve voltage regulation in low-voltage dc microgrids," *IEEE Transactions on Power Electronics*, vol. 28, no. 4, pp. 1900–1913, April 2013.

[21] J. Xiao, P. Wang, and L. Setyawan, "Hierarchical control of hybrid energy storage system in dc microgrids," *IEEE Transactions on Industrial Electronics*, vol. 62, no. 8, pp. 4915–4924, Aug 2015.

[22] Y. Hu, X. Wang, Y. Peng, J. Xiang, and W. Wei, "Distributed finite-time secondary control for dc microgrids with virtual impedance arrangement," *IEEE Access*, vol. 7, pp. 57 060–57 068, 2019.

[23] V. Nasirian, A. Davoudi, F. L. Lewis, and J. M. Guerrero, "Distributed adaptive droop control for dc distribution systems," *IEEE Transactions on Energy Conversion*, vol. 29, no. 4, pp. 944–956, Dec 2014.

[24] S. Peyghami, H. Mokhtari, and F. Blaabjerg, "Decentralized load sharing in a low-voltage direct current microgrid with an adaptive droop approach based on a superimposed frequency," *IEEE Journal of Emerging and Selected Topics in Power Electronics*, vol. 5, no. 3, pp. 1205–1215, Sep. 2017.

[25] M. Zaery, E. M. Ahmed, M. Orabi, and M. Youssef, "Operational cost reduction based on distributed adaptive droop control technique in dc microgrids," in *2017 IEEE Energy Conversion Congress and Exposition (ECCE)*, Oct 2017, pp. 2638–2644.

[26] B. Ko, G. Lee, K. Choi, and R. Kim, "A coordinated droop control method using a virtual voltage axis for power management and voltage restoration of dc microgrids," *IEEE Transactions on Industrial Electronics*, pp. 1–1, 2018.

[27] M. A. Mumtaz, M. M. Khan, F. Xianghong, A. Karni, and M. T. Faiz, "An improved cooperative control method of dc microgrids based on finite gain controller," in *2018 20th European Conference on Power Electronics and Applications (EPE'18 ECCE Europe)*, Sep. 2018, pp. P.1–P.9.

[28] J. Xiao, P. Wang, and L. Setyawan, "Multilevel energy management system for hybridization of energy storages in dc microgrids," *IEEE Transactions on Smart Grid*, vol. 7, no. 2, pp. 847–856, March 2016.

[29] Y. Yang, M. M. Khan, and J. Yu, "An improved cooperative control method of dc microgrid based on nearest neighbors communication," in *IECON 2017 - 43rd Annual Conference of the IEEE Industrial Electronics Society*, Oct 2017, pp. 792–797.

[30] S. Sahoo and S. Mishra, "A distributed finite-time secondary average voltage regulation and current sharing controller for dc microgrids," *IEEE Transactions on Smart Grid*, vol. 10, no. 1, pp. 282–292, Jan 2019.

[31] J. Hu, J. Duan, H. Ma, and M. Chow, "Distributed adaptive droop control for optimal power dispatch in dc microgrid," *IEEE Transactions on Industrial Electronics*, vol. 65, no. 1, pp. 778–789, Jan 2018.

[32] F. Chen, R. Burgos, D. Boroyevich, E. Rodriguez-Diaz, L. Meng, J. C. Vasquez, and J. M. Guerrero, "Analysis and distributed control of power flow in dc microgrids to improve system efficiency," in *2016 4th International Symposium on Environmental Friendly Energies and Applications (EFEA)*, Sep. 2016, pp. 1–6.

[33] S. Moayedi and A. Davoudi, "Unifying distributed dynamic optimization and control of islanded dc microgrids," *IEEE Transactions on Power Electronics*, vol. 32, no. 3, pp. 2329–2346, March 2017.

[34] X. Zhang, M. Dong, and J. Ou, "A distributed cooperative control strategy based on consensus algorithm in dc microgrid," in *2018 13th IEEE Conference on Industrial Electronics and Applications (ICIEA)*, May 2018, pp. 243–248.

[35] A. Ingle, A. B. Shyam, S. R. Sahoo, and S. Anand, "Quality-index based distributed secondary controller for a low-voltage dc microgrid," *IEEE Transactions on Industrial Electronics*, vol. 65, no. 9, pp. 7004–7014, Sep. 2018.

[36] F. Chen, R. Burgos, D. Boroyevich, J. Vasquez, and J. M. Guerrero, "Investigation of nonlinear droop control in dc power distribution systems: Load sharing, voltage regulation, efficiency and stability," *IEEE Transactions on Power Electronics*, pp. 1–1, 2019.

[37] E. G. Shehata, J. Thomas, R. M. Mostafa, and M. A. Ghalib, "An improved droop control for a low voltage dc microgrid operation," in *2018 Twentieth International Middle East Power Systems Conference (MEPCON)*, Dec 2018, pp. 850–855.

[38] N. Yang, D. Paire, F. Gao, A. Miraoui, and W. Liu, "Compensation of droop control using common load condition in dc microgrids to improve voltage regulation and load sharing," *International Journal of Electrical Power & Energy Systems*, vol. 64, pp. 752 – 760, 2015. [Online]. Available: http://www.sciencedirect.com/science/article/pii/S0142061514005237

[39] X. Liu, H. He, Y. Wang, Q. Xu, and F. Guo, "Distributed hybrid secondary control for a dc microgrid via discrete-time interaction," *IEEE Transactions on Energy Conversion*, vol. 33, no. 4, pp. 1865–1875, Dec 2018.

[40] F. Guo, L. Wang, C. Wen, D. Zhang, and Q. Xu, "Distributed voltage restoration and current sharing control in islanded dc microgrid systems without continuous communication," *IEEE Transactions on Industrial Electronics*, pp. 1–1, 2019.

[41] M. Tucci, L. Meng, J. M. Guerrero, and G. Ferrari-Trecate, "Stable current sharing and voltage balancing in dc microgrids: A consensus-based secondary control layer," *Automatica*, vol. 95, pp. 1 – 13, 2018. [Online]. Available: http://www.sciencedirect.com/science/article/pii/S0005109818302024

[42] W. W. A. G. da Silva, T. R. Oliveira, and P. F. Donoso-Garcia, "Hybrid distributed and decentralized secondary control strategy to attain accurate power sharing and improved voltage restoration in dc microgrids," *IEEE Transactions on Power Electronics*, vol. 35, no. 6, pp. 6458–6469, 2020.

[43] H. Wang, M. Han, J. M. Guerrero, J. C. Vasquez, and B. G. Teshager, "Distributed secondary and tertiary controls for i–v droop-controlled-paralleled dc–dc converters," *IET Generation, Transmission Distribution*, vol. 12, no. 7, pp. 1538–1546, 2018.

[44] S. Sahoo and S. Mishra, "An adaptive event-triggered communication-based distributed secondary control for dc microgrids," *IEEE Transactions on Smart Grid*, vol. 9, no. 6, pp. 6674–6683, Nov 2018.

[45] D. Pullaguram, S. Mishra, and N. Senroy, "Event-triggered communication based distributed control scheme for dc microgrid," *IEEE Transactions on Power Systems*, vol. 33, no. 5, pp. 5583–5593, Sep. 2018.